Transactions of the Materials Research Society of Japan 32[1] 209-214 (2007)

In-situ X-ray diffraction study of InAs/GaAs(001) quantum dot growth

Masamitu Takahasi, Toshiyuki Kaizu and Jun'ichiro Mizuki
Synchrotron Radiation Research Center, Japan Atomic Energy Agency,
Koto 1-1-1, Sayo-cho, Sayo-gun, Hyogo 679-5148
Fax: 81-791-58-2701, e-mail: mtaka@spring8.or.jp

Molecular beam epitaxial (MBE) growth of InAs/GaAs(001) quantum dots and their annealing after deposition were investigated by grazing-incidence X-ray diffraction using a diffractometer integrated with an MBE apparatus. Use of synchrotron radiation and a two-dimensional X-ray detector enabled X-ray diffraction intensity mapping in the reciprocal lattice space at a rate of less than 10 s per frame. Results suggest that the degree of alloying that depends on the growth temperature has a strong influence on the structural evolution during annealing.
Key words: X-ray diffraction, quantum dot, InAs, GaAs, molecular-beam epitaxy

1. INTRODUCTION

In heteroepitaxial growth of lattice-mismatched systems, strained epitaxial layers are known to be inherently unstable. Strains accumulated in a two-dimensional (2D) film are relieved by either formation of misfit dislocations at the interface or formation of islands on the surface. From the viewpoint of technological applications, Stranski Krastanow (SK) mode observed in a number of semiconductors, such as InGaAs/GaAs(001) [1], Ge/Si(001) [2], CdSe/ZnSe(001) [3] and PbSe/PbTe(111) [4], has attracted intense interest. In this growth mode, 3D nanometer-sized islands are spontaneously formed on a few monolayers (ML) of 2D wetting layers. The 3D islands formed in SK growth are dislocation-free single crystals with a narrow size distribution. Because these properties are desirable for quantum dot device applications, much work has been devoted to understand and control SK island growth. Since SK growth is a strain-driven process, it is essentially important to study strain fields inside SK islands. As growth temperature is raised, alloying takes place at the interface of heterostructures. It also changes strain energy and thus may contribute to strain relief at high temperatures.

Recently, several X-ray techniques have been developed to investigate a variety of structural properties of quantum dots. The dot shape was investigated by grazing-incidence small angle scattering [5–7] and intensity mapping in reciprocal space [8]. The strain distribution inside the dots was studied by thorough X-ray reciprocal space mapping [8–11] and by analysis of X-ray diffraction profiles [12]. The chemical composition in the dots was analyzed by utilizing X-ray anomalous scattering [13–17] and the structure factor of zinc-blende type crystals [8]. More recently, in-situ X-ray diffraction measurements have been carried out during InAs/GaAs(001) quantum dot growth [18,19]. These X-ray techniques are promising to reveal structural properties including internal strains and chemical compositions, which cannot be determined by conventional techniques including electron diffraction and scanning-probe microscopy.

The focus of the present work is strain evolution during annealing after deposition of a certain amount of InAs on GaAs(001). To get insight into the strain fields inside islands, we employed synchrotron X-ray diffraction. The highly collimated beam available from a synchrotron light source has enabled high resolution measurement of the strain fields. Further, measurement time has been so shortened with the help of large intensity of synchrotron X-rays that time-resolved measurements has become possible. We have compared annealing processes at various temperatures to examine the influence of alloying which is thermally enhanced.

2. EXPERIMENTAL

Experiments were carried out at a synchrotron experimental station, BL11XU of SPring-8, using a surface X-ray diffractometer integrated with an MBE apparatus [20]. The MBE chamber is equipped with X-ray windows made of beryllium along with five evaporation sources and a reflection high-energy electron diffraction (RHEED) system so that in situ X-ray diffraction measurements can be performed during MBE growth.

The samples were cut to a size of $7\times5\times0.3$ mm^3 from a commercially-supplied epi-ready wafer of GaAs(001). They were mounted on a molybdenum block with indium and loaded into the MBE cham-

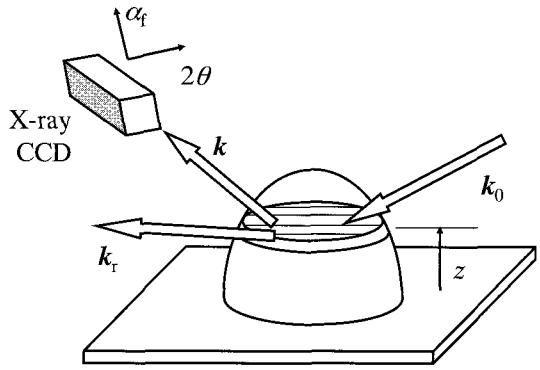

Fig. 1: Schematic of X-ray diffraction by a nanoisland grown on a substrate. The incoming beam, $\boldsymbol{k}_0$, is diffracted in the in-plane direction by crystallographic planes perpendicular to the substrate surface. The diffracted beam, $\boldsymbol{k}$, is detected by an X-ray CCD camera to measure the intensity distribution along the in-plane 2θ and the out-of-plane α_f directions. The intensity of the diffracted beam is proportional to the wave field at z generated by interference of the incoming beam, $\boldsymbol{k}_0$, and the reflected beam, $\boldsymbol{k}_r$.

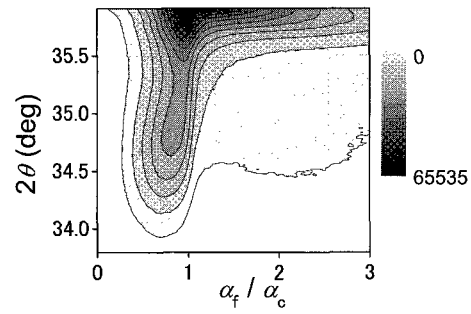

Fig. 2: Typical X-ray CCD image obtained from SK islands of InAs/GaAs(001). The measure sample is grown by depositing 2.5 monolayer InAs at a substrate temperature of 477°C.

ber. Following the thermal desorption of surface oxide layers and the growth of a 0.2-μm-thick buffer layer, the sample was cooled to a temperature for InAs growth. The As pressure was kept at 2×10^{-6} Torr during deposition of InAs and annealing. The substrate temperature was measured with an optical pyrometer which had been calibrated at the melting temperature of aluminum. The 2×4 reconstruction of the GaAs(001) surface was observed to change to $c(4\times4)$ at 480°C.

Figure 1 shows the schematic of the X-ray measurements. X-rays were monochromatized to be 1.24 Å by a Si(111) double-crystal system and focused by a pair of bent Pt-coated mirrors. The final beam size was determined by a Ta-blade slit to be 0.3 mm (horizontal) × 0.1 mm (vertical). The incident X-rays were diffracted by (220) planes of the nanoislands and the substrate. Since the (220) planes are perpendicular to the (001) surface, the momentum transfer is nearly parallel to the substrate surface. The angular distribution of the diffracted X-rays was measured with an X-ray charge coupled device (CCD) camera placed at a distance of 697.7 mm from the sample. The spatial resolution of the CCD was 0.1367 mm, which corresponds to the angular resolution of 0.01125°. The angular acceptance of the detector is limited to 4.3°by the aperture of an evacuated tube placed between the detector and the X-ray window. While the CCD was being exposed, the sample was rotated about the surface normal by 4°at a speed of 1.008°/s. By this method, the projection of the reciprocal space mapping onto the $(1\bar{1}0)$ plane was recorded in a single CCD image. The acquisition time of one frame was 9.6 s, including a readout time of about 5 s.

3. ANALYSIS

Figure 2 shows a typical X-ray CCD image. The horizontal axis represents the outgoing angle, α_f, which is normalized by the critical angle for total reflection of X-rays, α_c, and the vertical axis represents the in-plane scattering angle, 2θ. This image was obtained from the sample grown at a substrate temperature of 477°C. The amount of deposited InAs was 2.5 monolayers (ML).

Our analytical method is based on the iso-strain scattering described in Ref. [8]. In this treatment, a free-standing nanoisland is regarded as a stacking of iso-strain disks in which the in-plane lattice constant is uniform. Because the self-assembled SK islands are coherent crystals that are strained to match the substrate, the lattice constant inside the islands has a gradient in the vertical direction: the lattice constant of an iso-strain disk is the same as the substrate at the bottom of the island and is relaxed to be the intrinsic value of InAs near the top. Such a lattice constant distribution is observed as difference in 2θ.

In the framework of the distorted-wave Born approximation [21,22], the intensity of the diffraction from an iso-strain disk located at a height of z is modulated in proportion to the wave field at z. When the angle of incidence, α_i, is as small as the angle of the total reflection of X-rays, the interference between the incident and reflected waves results in the wave field expressed as

$$F(\alpha_i, z) = 1 + \frac{E_r}{E_i}\exp(2ik_\perp z), \qquad (1)$$

where E_i and E_r are the complex amplitudes of the incident and reflected X-rays, respectively, and $k_\perp = k\sin\alpha_i$ is the surface normal component of the wave vector of the incident X-rays. Note that

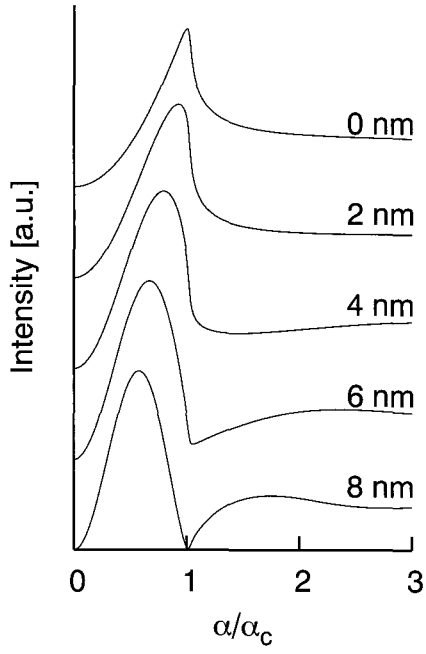

Fig. 3: Intensity of the wave field as a function of the incoming or outgoing angle for different heights measured from the substrate surface. The position that gives the maximum intensity is shifted to a smaller angle with increasing vertical distance from the substrate.

the amplitude and the phase of E_r vary as functions of the incident angle. In fact, the intensity of the diffracted beam depends on the outgoing angle as well. The reciprocity theorem in optics states that the optical phenomenon should be the same even if the source and observation points are exchanged. Owing to this theorem, the diffraction intensity from the iso-strain disks should be symmetric with respect to α_i and α_f. Therefore, the intensity distribution in the observed CCD image is given by

$$I(2\theta, \alpha_f) \propto |F(\alpha_i, z)|^2 |F(\alpha_f, z)|^2 S(2\theta), \quad (2)$$

where $S(2\theta)$ is the kinematical 2θ spectrum which is directly associated with the lattice constant distribution of the sample.

Figure 3 shows the calculation of $|F(\alpha, z)|^2$ for various z. The horizontal axis is normalized by α_c. The wave field formed over the surface is strongly modulated as a function of the glancing angle and its functional form depends on z.

There are two features of $|F(\alpha, z)|^2$ that will be exploited in the present work. Firstly, we focus on the angle giving the intensity maximum. While it coincides with α_c for $z = 0$, the peak position of $|F(\alpha, z)|^2$ is shifted to a smaller angle with increasing height from the substrate surface. Hence, from the angle of the maximum intensity, one can estimate the height at which the diffraction occurs and thus can determine the height of SK islands. Secondly, $|F(\alpha, z)|^2$ approaches to unity with increasing α irrespective of z. This is readily understood from Eq.(1) because the reflected wave, E_r, should be zero for $\alpha \to \infty$. Our interest is $S(2\theta)$ that is directly related to the lattice constant distribution. To derive $S(2\theta)$ from the measured intensity distribution, $I(2\theta, \alpha_f)$, we need to decouple 2θ and z in Eq.(2). If we assume that $|F(\alpha, z)|^2$ is unity at $\alpha = 3\alpha_c$, we obtain $I(2\theta, \alpha_i)/I(2\theta, 3\alpha_c) = |F(\alpha_i, z)|^2/|F(3\alpha_c, z)|^2 \simeq |F(\alpha_i, z)|^2$ from a measured CCD image. As a result, $S(2\theta)$ can be determined by $S(2\theta) \propto [I(2\theta, 3\alpha_c)]^2/I(2\theta, \alpha_i)$.

This procedure relies on the validity of the reciprocity theorem in optics. To make sure of the correctness of Eq.(2), we measured the diffraction intensity with changing either the incoming or the outgoing angle as shown in Figs. 4 (a) and (b). In Fig. 4(a), intensities at $\alpha_f = \alpha_c$ are plotted as a function of α_i for different 2θ. On the other hand, Fig. 4(b) shows the intensity profiles along α_f in a single CCD image measured at a fixed incoming angle of $\alpha_i = 0.2°$. The two results of Figs. 4(a) and (b) agree well, indicating that the symmetry with respect to α_i and α_f in Eq.(2) is true.

4. RESULTS AND DISCUSSION

Figures 5 (a), (b) and (c) show the temporal evolution of $S(2\theta)$ during the growth and annealing of InAs islands on GaAs(001) at temperatures of (a) 470°C, (b) 446°C and (c) 424°C. In these figures, 2θ is transformed to the relative lattice constant $\epsilon = a/a_{GaAs}$, where a and a_{GaAs} are the lattice constants of relaxed islands and the GaAs substrate, respectively. The number beside each curve denotes the time elapsed from the beginning of deposition. The curves are shifted vertically to avoid superposition. After deposition of 3 ML InAs, nucleated islands were annealed at the same temperature and in the same As flux. Measurements during InAs deposition and annealing were represented by dashed and solid lines, respectively.

The evolution of $S(2\theta)$ exhibits a significant temperature dependence. When InAs was deposited and annealed at 446°C, a peak developed at $\epsilon = 1.05$ during annealing. If the islands are matching the substrate, the lattice constant should distribute continuously from the value close to the substrate at the bottom of the islands to a fully relaxed value near the top. Hence we interpret the increase in intensity only at $\epsilon = 1.05$ as an indication of misfit dislocations. Similar peaks were found in the growth at 424°C. On the other hand, the peaks indicative of dislocations are indiscernible at 470°C. This behavior is reminiscent of the temperature dependence that has been observed in continuous growth of InAs [19], in which a bimodal lattice constant distribution is observed at 430°C as opposed to the growth at 480°C.

Figure 6 shows the change in SK dot height during annealing. While the height of islands stays constant during annealing at 470°C and 424°C, the is-

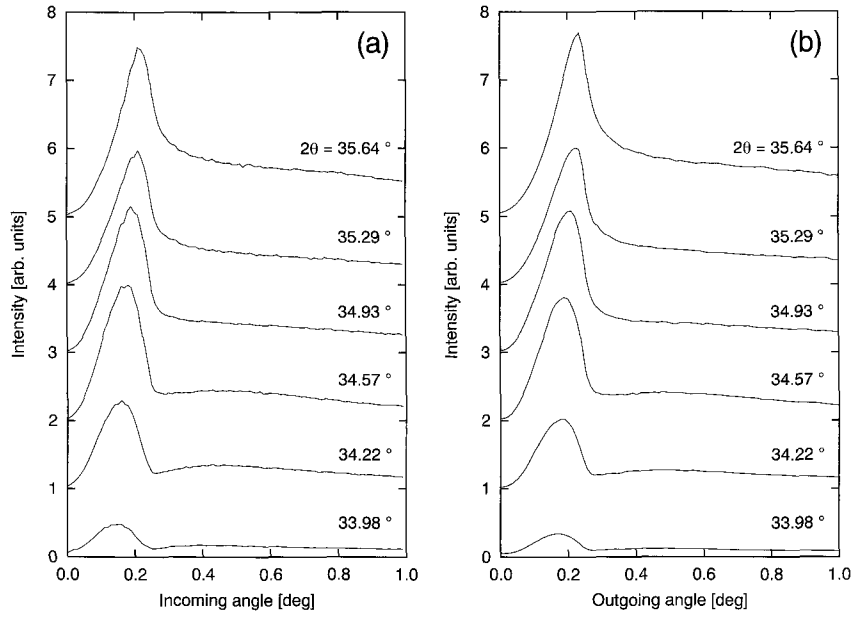

Fig. 4: Comparison of the diffraction intensity at fixed 2θ positions with changing incoming and outgoing angles. The intensity changes in the identical way as functions of the incoming and outgoing angles, indicating the validity of the reciprocity theorem in optics.

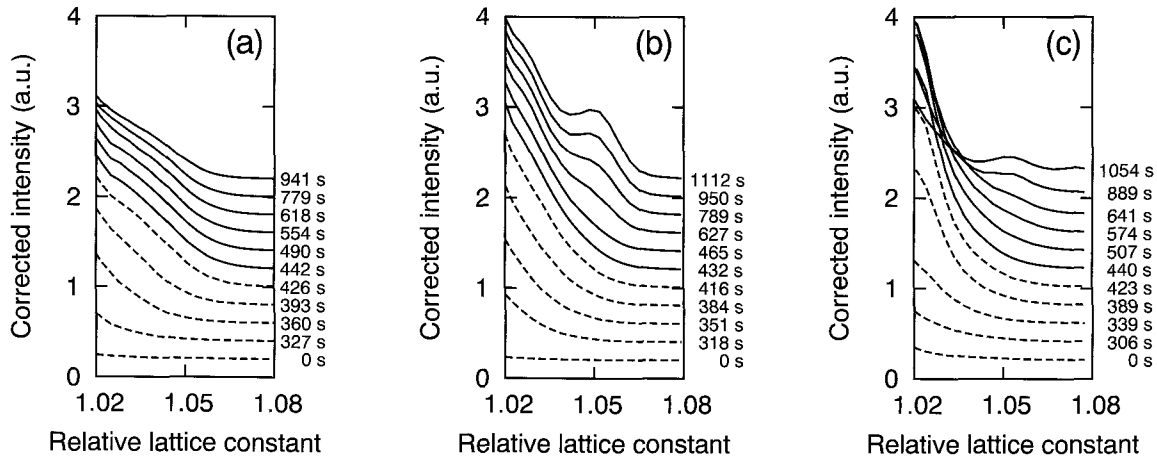

Fig. 5: Temporal evolution of the lattice constant distribution during growth (dashed lines) and annealing (solid lines) of InAs/GaAs(001) islands at temperatures of (a) 470°C, (b) 446°C and (c) 424°C.

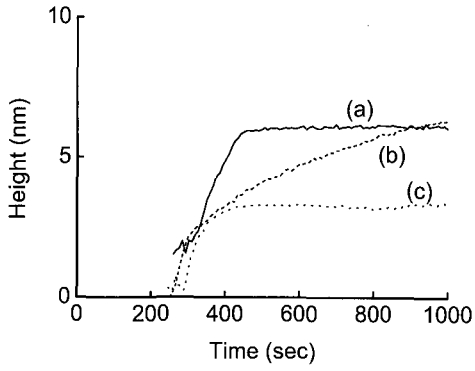

Fig. 6: Evolution of height during growth and annealing of InAs/GaAs(001) islands at temperatures of (a) 470°C, (b) 446°C and (c) 424°C. The deposition of InAs was stopped at 434 s, 432 s and 439 s for (a), (b) and (c), respectively.

lands keep growing at 446°C even after deposition of InAs was stopped at 432 s. The marked increase in height at 446°C is due to the formation of dislocated islands which are easier to coarsen than strained coherent islands. Strained islands do not tend to incorporate additional materials at the cost of the increase in elastic energy. This is why the islands grown at 470°C keep the initial height during annealing. At 424°C, on the other hand, mass transport through surface diffusion is suppressed. As a result, coarsening of islands is not significant even though dislocated islands are being formed over the course of annealing.

We ascribe the temperature-dependent structural change of SK islands to the degree of alloying. Recently, it has been revealed that InAs/GaAs(001) islands are more or less alloyed even if nominally pure InAs was deposited [8]. In general, alloying is enhanced at raised temperatures. The preference of coherent islands at 470°C suggests that, at this temperature, the strain energy can be relieved enough by alloying without invoking dislocations. In contrast, at such temperatures that alloying is thermally inhibited, islands are relaxed by generating dislocations. From our observations, the critical temperature determining whether dislocations are involved in strain relief or not seems to lie between 470°C and 446°C. We would like to discuss a relationship between this temperature range and the miscibility of InAs and GaAs. According to an estimation based on the thermodynamics, there is a miscibility gap of InAs and GaAs at temperatures below 482–500°C [23,24], which coincides with the critical temperature estimated in the present work. If the alloyed film is compressively strained to match the non-strained substrate, the temperature at which the miscibility gap is generated has been shown to become extremely low [25]. It is no wonder, however, that the calculation for the bulk can be applied to the SK islands because most part of the strain is relieved by forming islands. It should be noted that the discussion here premises that In and Ga can be redistributed in the islands during annealing. Although bulk diffusion is unlikely to occur at a typical growth temperature, a phenomenon called Ostwald ripening is known to take place commonly in many semiconductor quantum dot systems [1–4]. In this process, larger islands grow further at the expense of smaller islands, and thereby mass exchange among islands is enabled even when the bulk diffusion is negligible [26].

5. CONCLUSION

We investigated the strain evolution under MBE conditions using synchrotron X-ray diffraction. In situ observation with this technique revealed that structural change of InAs islands during annealing is governed by thermally-enhanced alloying.

REFERENCES

[1] B. D. Min, Y. Kim, E. K. Kim, S.-K. Min and M. J. Park, *Phys. Rev. B*, **57**, 11879-82 (1998).

[2] F. M. Ross, J. Tersoff and R. M. Tromp, *Phys. Rev. Lett.*, **80**, 984-7 (1998).

[3] H. Lee, R. Lowe-Webb, W. Yang and P. C. Sercel, *Appl. Phys. Lett.*, **72**, 812-14 (1998).

[4] A. Raab and G. Springholz, *Appl. Phys. Lett.*, **77**, 2991-3 (2000).

[5] M. Schmidbauer, T. Wiebach, H. Raidt, M. Hanke, R. Köhler and H. Wawra, *Phys. Rev. B*, **58**, 10523-31 (1998).

[6] M. Rauscher, R. Paniago, H. Metzger, Z. Kovats, J. Domke, J. Peisl, H.-D. Pflannes, J. Schulze and I. Eisele, *J. Appl. Phys.*, **86**, 6763-9 (1999).

[7] H. Okuda, S. Ochiai, K. Ito and Y. Amemiya, *Appl. Phys. Lett.*, **81**, 2358-60 (2002).

[8] I. Kegel, T. H. Metzger, A. Lorke, J. Peisl, J. Stangl, G. Bauer, K. Nordlund, W. V. Schoenfeld and P. M. Petroff, *Phys. Rev. B*, **63**, 035318-1-13 (2001).

[9] A. A. Darhuber, P. Schittenhelm, V. Holý, J. Stangl, G. Bauer and G. Abstreiter, *Phys. Rev. B*, **55**, 15652-63 (1997).

[10] T. Wiebach, M. Schmidbauer, M. Hanke, R. Köhler and H. Wawra, *Phys. Rev. B*, **61**, 5571 (2000).

[11] T. Uragami, A. S. Acosta, H. Fujioka, T. Mano, J. Ohta, H. Ofuchi, M. Oshima, Y. Takagi, M. Kimura and T. Suzuki, *J. Cryst. Growth*, **234**, 197-201 (2002).

[12] A. J. Steinfort, P. M. L. O. Scholte, A. Ettema, F. Tuinstra, M. Nielsen, E. Landemark, D.-M. Smilgies, R. Feidenhans'l, G. Falkenberg, L. Seehofer and R. L. Johnson, *Phys. Rev. Lett.*, **77**, 2009-12 (1996).

[13] T. U. Schülli, M. Sztucki, V. Chamard and T. H. Metzger, *Appl. Phys. Lett.*, **81**, 448-50 (2002).

[14] A. Malachias, S. Kycia, G. Medeiros-Riberio, R. Magalhães-Paniago, T. I. Kamins and R. S. Williams, *Phys. Rev. Lett.*, **91**, 176101-1-4 (2003).

[15] T. U. Schülli, J. Stangl, Z. Zhong, R. T. Lechner, M. Szucki, T. H. Metzger and G. Bauer, *Phys. Rev. Lett.*, **90**, 066105-1-4 (2003).

[16] V. Chamard, T. Schülli, M. Sztucki, T. H. Metzger, E. Sarigannidou, J.-L. Rouviére, M. Tolan, C. Adelmann and B. Daudin, *Phys. Rev. B*, **69**, 125327-1-8 (2004).

[17] A. Létoublon, V. Favre-Nicolin, H. Renevier, M. G. Proietti, C. Monat, M. Gendry, O. Marty and C. Priester, *Phys. Rev. Lett.*, **92**, 186101-1-4 (2004).

[18] M. Takahasi and J. Mizuki, *J. Cryst. Growth*, **275**, e2201-6 (2005).

[19] M. Takahasi, T. Kaizu and J. Mizuki, *Appl. Phys. Lett.*, **88**, 101917-1-3 (2006).

[20] M. Takahasi, Y. Yoneda, H. Inoue, N. Yamamoto and J. Mizuki, *Jpn. J. Appl. Phys.*, **41**, 6247-51 (2002).

[21] G. H. Vineyard, *Phys. Rev. B*, **26**, 4146-59 (1982).

[22] S. K. Shinha, E. B. Shirota, S. Garoff and H. B. Stanley, *Phys. Rev. B*, **38**, 2297-311 (1988).

[23] K. Onabe, *Jpn. J. Appl. Phys.*, **21**, 964 (1982).

[24] S. Vannarat, M. H. F. Sluiter and Y. Kawazoe, *Jpn. J. Appl. Phys.*, **41**, 2536-41 (2002).

[25] D. Schlenker, T. Miyamoto, Z. Chen, M. Kawaguchi, T. Kondo, E. Gouardes, J. Gemmer, C. Gemmer, F. Koyama and K. Iga, *Jpn. J. Appl. Phys.*, **39**, 5751-57 (2000).

[26] U. Denker, A. Rastelli, M. Stoffel, J. Tersoff, G. Katsaros, G. Costantini, K. Kern, N. Jin-Phillipp, D. E. Jesson and O. G. Schmidt, *Phys. Rev. Lett.*, **94**, 216103-1-4 (2005).

(Received December 9, 2006;Accepted February 5, 2007)